Deformation and Fracture of Lamellar and Cylindrical Block Copolymers with Unentangled Glassy Matrices: Effect of Chain Architecture and Microdomain Orientation

Vikram Khanna,[†] Janne Ruokolainen,[†,§] Edward J. Kramer,*[,†] and Stephen F. Hahn[‡]

Department of Materials, University of California, Santa Barbara, Santa Barbara, California 93106, and Corporate R&D, Performance Plastics and Chemicals, The Dow Chemical Company, Freeport, Texas 77541

Received March 2, 2006; Revised Manuscript Received April 4, 2006

ABSTRACT: We investigate the influence of chain architecture and microdomain orientation on the deformation and fracture properties of relatively thick films (600−800 nm) of poly(cyclohexylethylene)−poly(ethylene) (PCHE−PE) block copolymers with various architectures. Optical microscopy, transmission electron microscopy, and scanning force microscopy are used to study the domain structure as well as examine the details of deformation and fracture of films stretched on ductile copper grids. For lamellar block copolymers the deformation and fracture properties depend significantly on the chain architecture. Annealed diblock copolymer films containing 48% PE show 100% failure at very low strains of 5% with a median strain to failure of 2%, whereas the lamellar triblock (CEC) and pentablock copolymer (CECEC) films do not fail at strains up to 27%. However, a 50/50 blend of diblock (CE $M_W = 22$ kg/mol, $f_{PE} = 0.48$) and triblock (CEC $M_W = 45$ kg/mol, $f_{PE} = 0.48$) copolymers shows a median strain to failure of about 6.4%. A 50/50 blend of the same diblock and pentablock (CECEC $M_W = 66$ kg/mol, $f_{PE} = 0.48$) copolymers, on the other hand, does not show any failure at strains up to 27%. Experiments on a cylinder-forming pentablock copolymer (CECEC $M_W = 60$ kg/mol, $f_{PE} = 0.25$) with slow ordering kinetics show that the maximum ductility with no failure at the maximum strain of 27% is obtained if the PE cylinders are randomly oriented (spun-cast films). Films having cylinders that are aligned parallel as well as perpendicular to the tensile direction (annealed for 3 days with cylinders lying down in the plane of the film) show a reduction in ductility with 30% failure at the maximum strain. As the proportion of cylinders aligned perpendicular to the tensile direction is increased (by increasing the annealing time to 7 days, the top half of the film shows cylinders that align normal to the film plane), 100% of the film squares fail at the maximum strain of 27% with a median strain to failure of about 19%. Moreover, in a film half as thick (∼300 nm), after a 7 day anneal, the perpendicular orientation persists throughout the film thickness. This sample shows complete failure at about 22% strain with a median strain to failure of about 15.7%. These results indicate that the orientation of the cylinders in the films has a strong effect on the mechanical properties of this pentablock copolymer, similar to conclusions reached previously for the triblock copolymer architecture. The results obtained in these studies are compared with those reported in previous works for the same system to ascertain the relative effect of chain architecture, microdomain orientation, and composition on the mechanical behavior of the block copolymer thin films.

Introduction

Glassy amorphous polymers exhibit desirable characteristics such as excellent optical clarity, low density, and easy processability, thereby making them ideal candidates for engineering applications. However, they are often extremely brittle due to their high entanglement molecular weight (M_e) (low entangled strand density).[1] The deformation mechanism as well as the extensibility of a glassy polymer is influenced strongly by its network structure, namely entanglements and cross-links. Films of polymeric networks with a high entangled strand density or a high cross-link density tend to form shear deformation zones. Fracture rarely initiates in such shear deformation zones.[2] On the other hand, a low entangled strand density (high M_e) predisposes the polymer to form weak crazes with high extension ratios and lower volume fractions of craze fibrils, which subsequently undergo premature failure. Hence, the molecular weight of a polymer needs to be far above its M_e in order for it to be useful for any structural applications. Since processability of high molecular weight polymers is not an easy task, other alternatives are desirable. Addition of rubber particles to the polymer matrix is a method that has been successfully employed in the past to overcome this inherent brittleness for glassy polymers.[3] However, this gain in mechanical toughness is offset by a loss in optical properties due to the refractive index mismatch of the matrix and the large rubber particles.[4] Hence, for applications requiring high transparency, this method has a serious drawback.

Block copolymers, containing a glassy and a rubbery block, have the ability to relieve the undesirable brittleness of glassy homopolymers, while retaining their desirable optical characteristics.[5] The mesoscopic self-assembly of the block copolymer in the molten and solid state, driven by chemical immiscibility between the different blocks,[5] gives rise to a variety of microphase-separated structures with a typical domain size of 5−100 nm. Optical homogeneity of the block copolymer can be ensured if the domain size is small enough. In addition, a rubbery block with a low M_e can circumvent the predisposition to failure of unentangled glassy polymers. However, proper design of block copolymers is essential for the development of useful materials that will satisfy the requisite criteria for specific

* To whom correspondence should be addressed: e-mail edkramer@mrl.ucsb.edu; Tel (805) 893-4999.
[†] University of California, Santa Barbara.
[‡] The Dow Chemical Company.
[§] Present address: Helsinki University of Technology, Department of Engineering Physics, P.O. Box 2200, FIN-02015 HUT, Finland.

10.1021/ma060460y CCC: $33.50
Published on Web 05/28/2006

applications. Molecular weight, composition, morphology, chain architecture, orientation of the microdomains, and thermal history of the block copolymer are the main factors that determine its final mechanical properties. Early work by Matsuo et al. on the mechanical properties of polystyrene−polybutadiene (PS−PB) block copolymers showed that triblock (SBS) and tetrablock (SBSB) copolymers were ductile, whereas diblock (SB) and triblock (BSB) copolymers with the glassy block in the middle were brittle.[8] In a series of papers, Weidisch and co-workers have shown that the block copolymer morphology and composition have a strong influence on the mechanical properties of poly(styrene-*b*-butyl methacrylate) (PS−PBMA) diblock copolymers. They observed that the mechanical properties of PS−PnBMA (26% PnBMA) are better than that of pure PS homopolymer,[9] and microphase-separated block copolymers show a considerable improvement over disordered block copolymers which exhibit a mechanical behavior that is similar to pure PS.[10] They also compared the mechanical behavior of different morphologies and reported that diblock copolymers with bicontinuous structures (39% PS) are tougher than diblock copolymers with a lamellar morphology (50% PS).[9] Another work reported the effect of the strength of segregation (χN) on the mechanism of deformation.[11] Recently, they have also reported a transition in deformation mechanisms from crazing to shear deformation with a change in architecture from triblock to star block.[12] In a recent work, Adhikari and Michler have examined the effect of molecular architecture on the phase and mechanical behavior of amorphous styrene/butadiene diblock copolymers.[13] By keeping the molecular weight and composition constant and changing the chain architecture, they were able to adjust the mechanical response over a wide range and study a variety of micromechanical deformation mechanisms in different morphologies.

Poly(cyclohexylethylene) is a glassy amorphous polymer that has excellent optical properties with desirable thermal characteristics. Excellent clarity, UV stability, low birefringence, and a high glass transition temperature T_g (= 145 °C) make it a promising candidate for industrial applications.[14] However, it is extremely brittle due to its high entanglement molecular weight (49 000 g/mol).[14] To circumvent the problem of brittleness of the homopolymer, poly(cyclohexylethylene)−poly(ethylene) (PCHE−PE) block copolymers can be designed. Such block copolymers are capable of segregating at the nanoscale level into cylindrical or lamellar morphology. Previously, Ryu et al. have shown that PCHE−PE cylinder-forming triblock copolymers show moderate improvement in the mechanical properties relative to the glassy homopolymer. However, when the chain architecture is changed from triblock to pentablock, keeping the molecular weight and composition constant, a brittle to ductile transition is observed.[15] They attributed this enhancement in toughness to the presence of a glassy C midblock between the two rubbery E blocks. Ruokolainen et al. then investigated the effect of thermal history and microdomain orientation on the deformation and fracture of cylindrical PCHE−PE triblock copolymer (CEC) films.[16] They observed that the behavior was strongly dependent on the amount of physical aging in the glassy PCHE domains and on the orientation of the PE microdomains. A random or parallel orientation of the cylinder axes relative to the direction of strain produced a more ductile behavior as compared to a perpendicular orientation. Also, elimination of physical aging enhanced the toughness of the block copolymers. However, crystallization conditions of the PE block do not affect the mechanical properties of the block copolymer. Hermel et al.[17] compared the mechanical behavior of shear aligned bulk CEC and CECEC lamellar block copolymers. They observed that when the strain is applied in a direction perpendicular to the lamellar normal, the triblock shows a brittle response whereas the pentablock exhibited a ductile behavior. They attributed the difference in the behavior to the presence of C midblocks between the E domains. They hypothesized that for the triblock the brittle failure occurs through the glassy PCHE domains. The pentablock deforms with the onset of shear yielding in the PE domains, followed by necking and drawing and finally strain hardening before rupture. Mori et al.[18] studied the mechanical behavior of bulk samples of a blend of a triblock and pentablock and found that addition of just 10 wt % of the pentablock to the triblock results in a dramatic improvement in the mechanical response of the triblock when stretched in a direction perpendicular to the lamellae normal.

The aim of this work is to achieve a complete understanding of the factors affecting the mechanical behavior of these block copolymers by investigating two more factors affecting the mechanical properties. In the first part, the effect of chain architecture in films of lamellar block copolymers is investigated. The deformation mechanisms and fracture statistics for the various architectures are discussed, and an attempt is made to understand the differences in the micromechanical behavior based on the structure of the block copolymers. In the second part, the effect of microdomain orientation on the mechanical properties of cylindrical PCHE−PE pentablock copolymer (CECEC) is investigated. A slow change in orientation of the pentablock cylinder microdomains is observed with annealing time, from a random orientation to one perpendicular to the film surfaces. Our results suggest that even for the tough pentablock architecture, differences in the mechanical behavior are observed with changes in microdomain orientation. The results obtained in this work are compared and related to the data from previous work in order to obtain a more comprehensive picture of the mechanical behavior of this block copolymer system.

Experimental Procedures

Materials and Film Preparation. The PCHE−PE block copolymers were synthesized at the Dow Chemical Company. The synthesis involved heterogeneous catalytic hydrogenation of polystyrene−polybutadiene (PS−PB) block copolymer precursors.[19] After hydrogenation, the PE blocks contained an average of 26 ethyl branches per 1000 backbone carbons. This was due to the 10% 1,2 monomer addition in the PB block. The polyethylene weight fraction was 0.48 for the lamellar block copolymers and 0.25 for the cylindrical ones. For the sake of convenience, a nomenclature is adopted for the different block copolymers where the C refers to the poly(cyclohexylethylene) block and E corresponds to the poly(ethylene) block. Hence, CE stands for a diblock copolymer and CEC stands for a triblock copolymer with a poly(ethylene) midblock. The names are followed by a 4 digit number. The first 2 digits indicate the M_W in kg/mol, and the next 2 give the weight fraction of poly(ethylene) in the block copolymer. As an example, $CEC_{45.48}$ is a 45 kg/mol triblock copolymer containing 48% poly(ethylene). The molecular weights and composition of the block copolymers used in this study are listed in Table 1.

Uniform thin films of the block copolymer were spun-cast from hot decahydronaphthalene solutions on hot NaCl substrates at 2500 rpm for 40 s. The temperature of the substrate was maintained at 120 °C using an IR lamp with a voltage regulator. The resulting films were about 600 nm thick for the cylindrical block copolymer and about 800 nm thick for the lamellar block copolymers. The

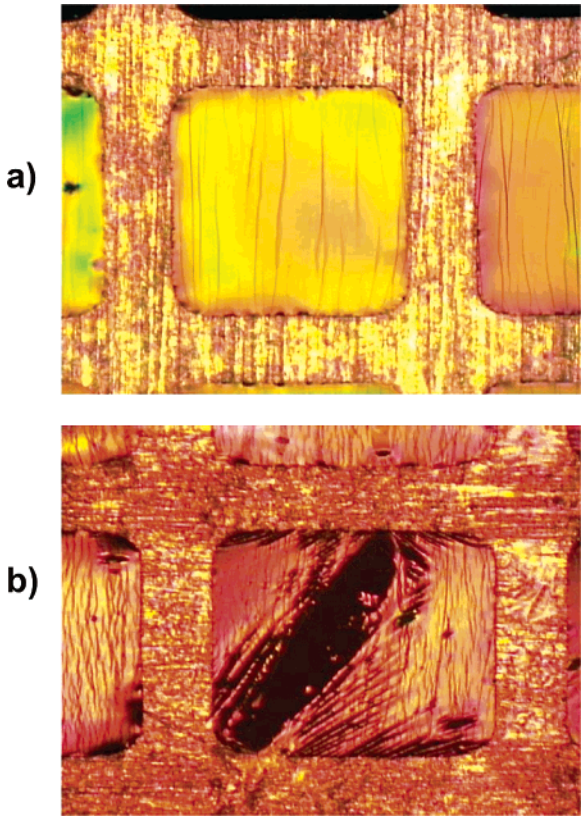

Figure 1. Typical reflective optical microscopy images of block copolymer films under tension depicting (a) deformation and (b) failure.

Table 1. Molecular Weight, Composition, Block Length, Annealing Temperature, and Annealing Time of the Poly(cyclohexylethylene)−Polyethylene Block Copolymers

polymer	chain architecture	M_W (kg/mol)	f_{PE} (wt %)	PCHE block (g/mol)	annealing temp (°C)	annealing time (days)
$CE_{22.48}$	diblock	22	48	11 400	220	3
$CEC_{45.48}$	triblock	45	48	11 250	220	3
$CECEC_{66.48}$	pentablock	66	48	11 450	220	3
$CECEC_{60.25}$	pentablock	60	25	15 000	180	3, 7

higher viscosity of the lamellar block copolymer solutions due to the higher weight fraction of PE, the poorly solvated block, results in thicker films. The block copolymer films were then annealed at a specific temperature for the required time (see Table 1). The annealing was done under a vacuum of about 10^{-8} mbar. The specific annealing temperature was chosen such that it was sufficiently above the glass transition temperature of the glassy PCHE block but below the order−disorder transition temperatures of the block copolymers. Since the glass transition temperature of the PCHE is 145 °C, the chosen temperature ensures that the block copolymer is ordered in the melt before the glassy matrix vitrifies. The films were allowed to cool slowly to the T_g of the glassy block and then were quenched to room temperature to avoid any physical aging.

Fragility Tests. The copper grid technique was used to investigate the deformation and fracture mechanisms of the block copolymers.[1] Annealed films were floated off the NaCl substrates onto the surface of a water bath. The films were picked up on ductile copper grids which had been previously annealed at 600 °C for 10 min and dip-coated with a thin layer of PCHE homopolymer. To bond the film to the homopolymer coating on the grid, a short exposure of the mounted film to toluene vapor was carried out. This ensures uniform bonding of the film around the periphery of each grid square. This exposure also relaxes some of the biaxial orientation in the film. This causes the film to shrink in area and pull taut over each grid square. The residual toluene vapor was

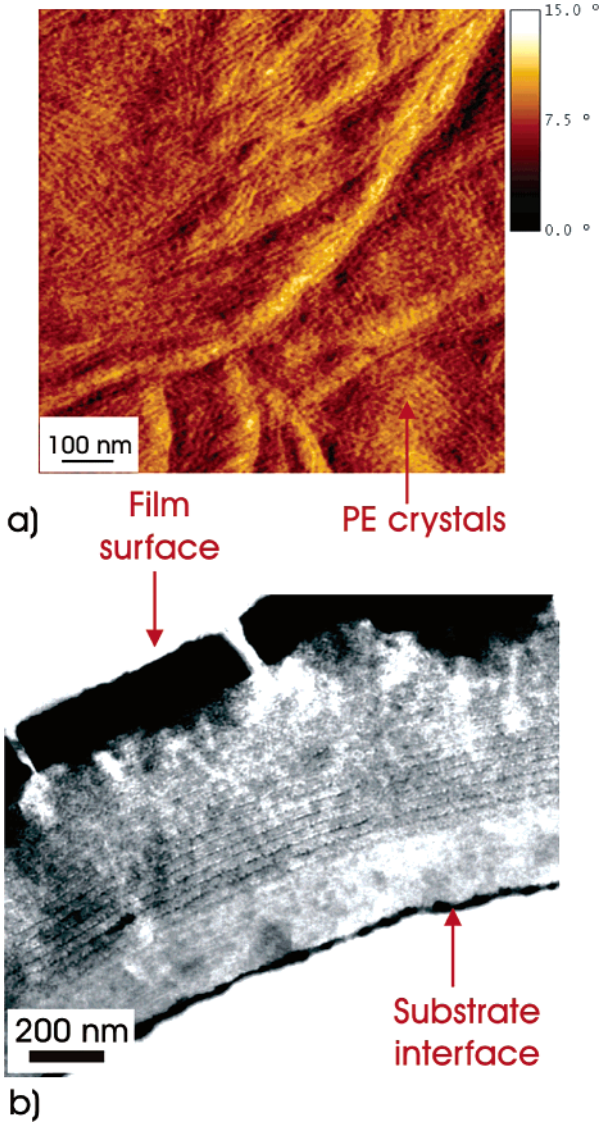

Figure 2. (a) Tapping mode SFM phase image and (b) cross-sectional TEM image of $CE_{22.48}$ annealed at 220 °C for 3 days.

removed by drying the bonded film squares under vacuum overnight. The films bonded to the copper grid were subsequently deformed under tension at room temperature. Depending on the film size and sample preparation, each copper grid contained about 25−35 individual polymer film squares. The polymer films were deformed using a translation stage equipped with a motor and gear head. The strain rate was adjusted to be about 1×10^{-4} s^{-1}. Periodic inspection of each grid square under tension was carried out using reflection optical microscopy to obtain information about craze initiation and failure (Figure 1). Since individual film squares undergo deformation independent of adjacent film squares, a reliable statistical analysis was possible. The results from the fragility tests reported in this paper were an average of four copper grid experiments for each sample.

Scanning Force Microscopy (SFM). To characterize the domain structures of the microphase-separated block copolymers, scanning force microscopy measurements were performed using a Digital Instruments Dimension 3000 and a Digital Instruments Nanoscope IIIa. The microscopes were operated in tapping mode. TESP tips by Nanodevices, which have a tip radius of ~10 nm and a spring constant of ~40 N/m, were used for the scans. The SFM was operated at the resonant frequency of the TESP tip (150−180 kHz). The highest quality images were obtained under soft tapping conditions at a scan rate of 1 Hz and a resolution (the number of pixels per line) of 512 pixels. The mechanical and height contrast

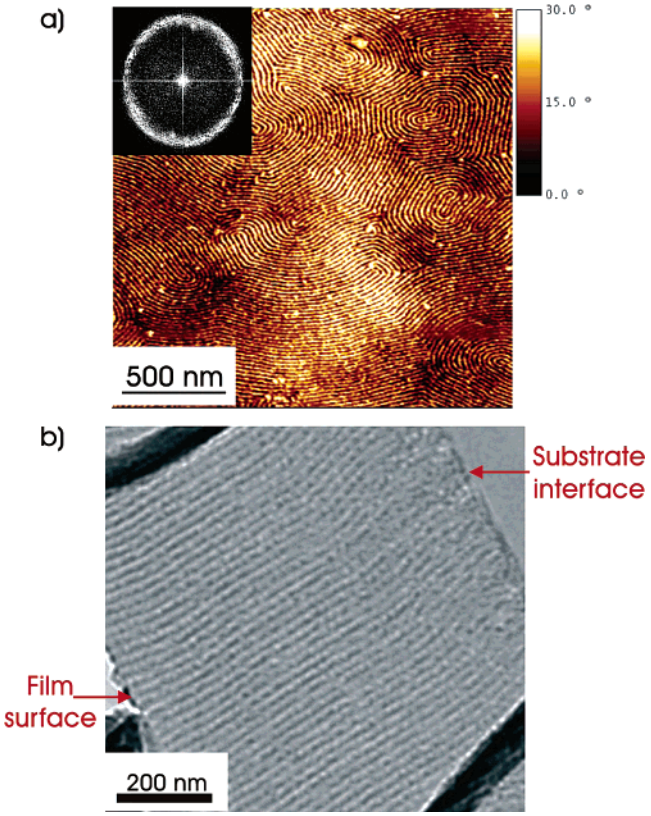

Figure 3. (a) Tapping mode SFM phase image and (b) cross-sectional TEM image of $CEC_{45.48}$ annealed at 220 °C for 3 days. The associated FFT for the SFM image, which is a ring, is shown in the inset. The ring suggests that there are no preferred orientations for the lamellar sheets in the film plane.

between the glassy PCHE and softer PE domains enables the imaging of the microphase-separated domains of the polymer films.[20] Both height and phase images are obtained for the block copolymer films. However, since better phase contrast is obtained for this system, only phase images are reported in this study.

Transmission Electron Microscopy (TEM). The copper grid technique also enables the structural investigation of the highly deformed regions of the block copolymer using transmission electron microscopy. Following the fragility test, a typical grid square is cut from the copper grid using a razor blade and examined using TEM. The plastically deformed copper grid holds the film under tension during TEM imaging since the polymer film is bonded to the grid square.

Cross-sectional TEM of the films was done in order to characterize the orientation of the microdomains. The films were floated off the NaCl substrates onto epoxy substrates. The films were then stained in RuO_4 vapor for 20 h using a stabilized 0.5% RuO_4 aqueous solution, obtained from Electron Microscopy Sciences. This was followed by capping of the films with another layer of epoxy. Film sections of 100 nm thickness were microtomed at room temperature using a Leica Ultracut UCT ultramicrotome and a diamond knife. The cross sections were imaged using an FEI-T20 TEM operated at 200 keV. Different degrees of staining of the amorphous PE regions, the PE crystals, and the glassy PCHE matrix by RuO_4 vapor enables the necessary imaging contrast in the TEM.[23]

Electron Microscopy Image Analysis. An important determinant of craze fibril stability is the craze fibril volume fraction ν_f or its inverse λ_{craze}, the craze extension ratio.[1] The craze is observed to widen by surface drawing while it preserves a constant λ, a process similar to the cold drawing of a macroscopic fiber. Hence, the craze extension ratio is the analogue of the so-called natural draw ratio of the fiber. Brown[21] and Lauterwasser and Kramer[22] independently developed a method to measure the craze extension

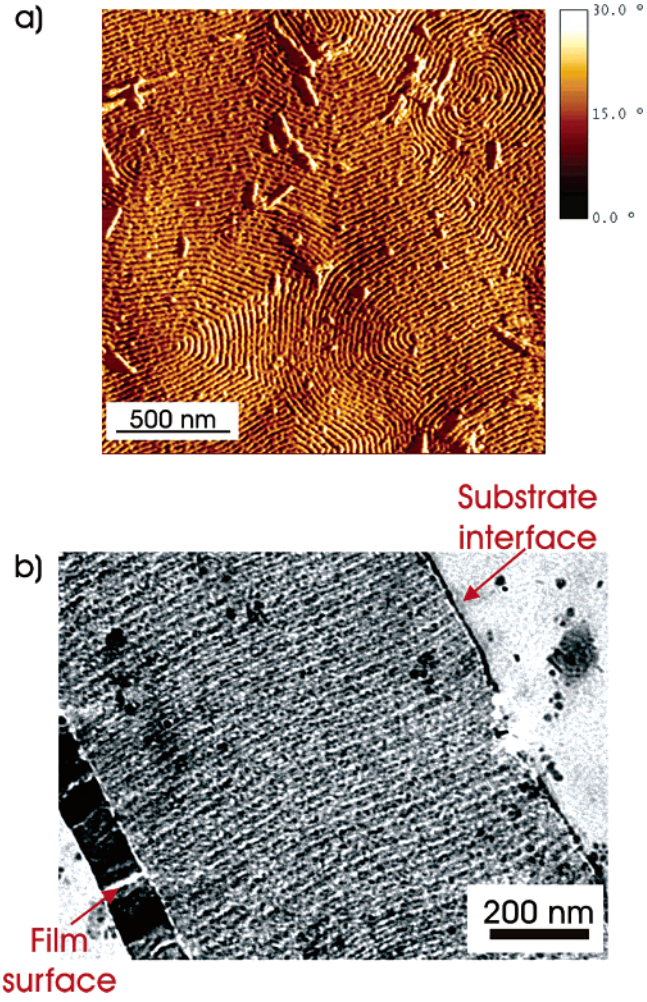

Figure 4. (a) Tapping mode SFM phase image and (b) cross-sectional TEM image of $CECEC_{66.48}$ annealed at 200 °C for 3 days.

ratio (λ_{craze}) from measurements of the optical densities on the electron image plates. The method is based on the principle that in TEM the electron beam current density imaged after passing through the objective aperture is exponentially attenuated according to the thickness and density of the polymer located along its path (mass−thickness contrast). If the exposure time of the image is adjusted to fall within the linear response regime of the sensitivity of the electron image plate, the optical density produced in the emulsion on the image plate is linearly proportional to the electron-beam current density. After obtaining the optical densities of the craze (ϕ_{cr}), the film (ϕ_f), and a hole in the film (ϕ_h) from the electron image plate locally, the relationship

$$\nu_f = \frac{1}{\lambda_{craze}} = 1 - \frac{\ln(\phi_{cr}/\phi_f)}{\ln(\phi_h/\phi_f)} \quad (1)$$

gives ν_f or λ_{craze}.

Results and Discussion

Effect of Chain Architecture on the Mechanical Behavior of Lamellar Block Copolymers Films. *Block Copolymer Morphology.* Three different architectures (diblock, triblock, and pentablock) with symmetric compositions ($f_E = 0.48$) were used in this study (see Table 1 for M_Ws, annealing temperatures, and times). The block copolymer morphology was investigated using scanning force microscopy and transmission electron microscopy. The three block copolymers have a lamellar morphology. The diblock copolymer, however, shows PE crystals on the

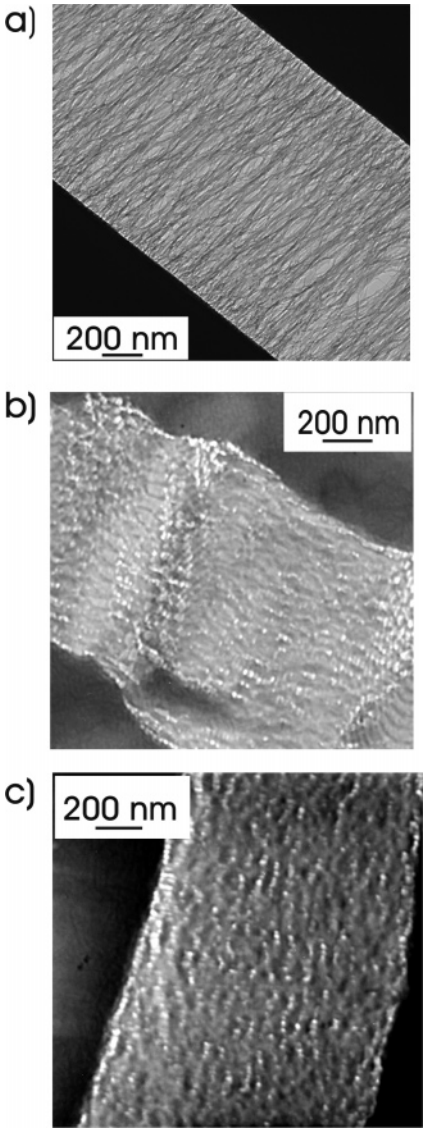

Figure 5. TEM images of typical deformed regions in (a) $CE_{22.48}$, (b) $CEC_{45.48}$, and (c) $CECEC_{66.48}$. Image a depicts a typical craze at 3% strain. Images b and c depict deformation zones with minimum voiding and were taken at 10% strain.

surface (Figure 2a), which suggests that the sheets might be oriented parallel to the film plane. TEM images show that this orientation persists throughout the film thickness (Figure 3b). SFM images for the triblock (Figure 3a) and the pentablock (Figure 4a) show that, on the surface, the lamellar sheets are aligned perpendicular to the plane of the film. However, as the Fourier transform (FFT) of the SFM image shows in Figure 3a, the lamellar sheets do not have any preferred orientation in the film plane. TEM images show that the perpendicular orientation persists throughout the film thickness (Figure 3b and 4). This unusual equilibrium orientation is caused by the entropic penalty for looping of the lower surface energy midblock in the parallel orientation coupled with the small difference in surface energies between the PCHE and PE blocks. The perpendicular orientation in the triblock and pentablock architectures thus has the lowest free energy. Since no looping is necessary to have the low surface energy PE on the surface in the diblock architecture, the parallel orientation is the lowest free energy state in this case and persists throughout the film thickness. The ordering behavior of the microdomains for this

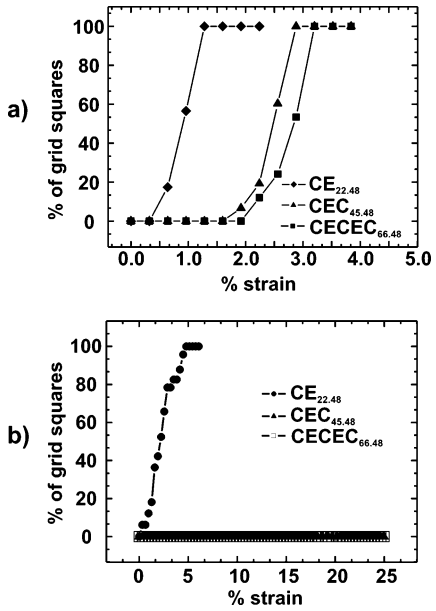

Figure 6. Cumulative number fraction of film squares that have (a) crazed and (b) failed as a function of strain for $CE_{22.48}$, $CEC_{45.48}$, and $CECEC_{66.48}$.

system has been discussed in more detail in another paper submitted for publication.

Deformation Mechanisms and Fracture Statistics. The morphology of plastically deformed regions of films with different architectures was investigated using the TEM procedure described in the Experimental Section. All the samples undergo deformation prior to failure. Figure 5a−c shows typical deformed regions for the diblock, triblock, and the pentablock architecture. The deformation and fracture statistics of the three individual block copolymers (CE, CEC, and CECEC) were determined using the fragility tests (Figure 6a,b).

The median strain to plastic deformation for the $CEC_{45.48}$ triblock and the $CECEC_{66.48}$ pentablock copolymers are 2.5% and 2.9%, respectively (Figure 6a). They deform predominantly by shear deformation with very little voiding in the deformed regions (Figure 5b,c). The extension ratios of the deformation zones for the CEC and CECEC block copolymer were calculated to be about 2.9 using the image analysis described in the Experimental Section. This value for the deformation zones is slightly lower than the value that was reported for the extension ratio of the deformation zones in a high-M_W cylinder-forming pentablock copolymer $CECEC_{110.30}$.[15] The difference may be due to the coexistence of the crazes and deformation zones for the latter (due to the lower weight fraction of the ductile PE phase).

$CEC_{45.48}$ and $CECEC_{66.48}$ both exhibit an extremely ductile behavior and do not show any failure prior to the end of the test (Figure 6b). For these two block copolymers, there is no observable effect of the chain architecture because the tests are limited by the ductile fracture of the Cu grid at about 27% strain. These low strains are not sufficient to cause failure in the lamellar triblock and pentablock copolymers. The high content of the highly entangled, ductile PE phase and the block copolymer architecture is likely to be responsible for their ductile behavior. CEC and CECEC block copolymers have glassy PCHE blocks at the end. The glassy C end blocks act as physical cross-links for the highly entangled and ductile E phase. Previous studies on the SBS system have shown that as compositional symmetry is approached and the PS and PB form

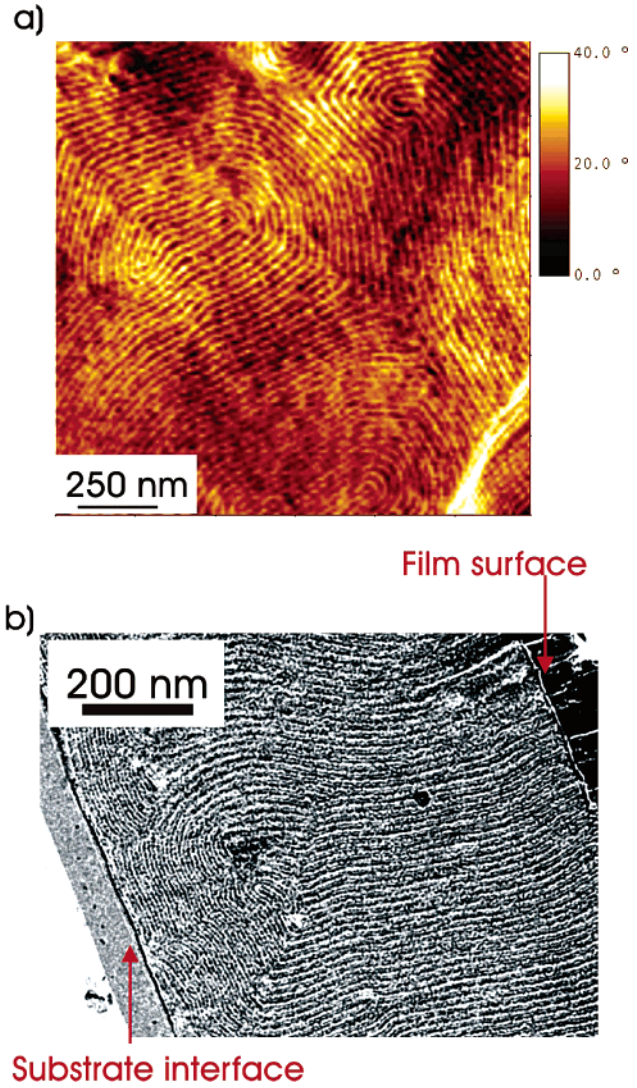

Figure 7. (a) Tapping mode SFM phase image and (b) cross-sectional TEM image of a symmetric blend $CEC_{45.48}/CE_{22.48}$ annealed at 220 °C for 3 days.

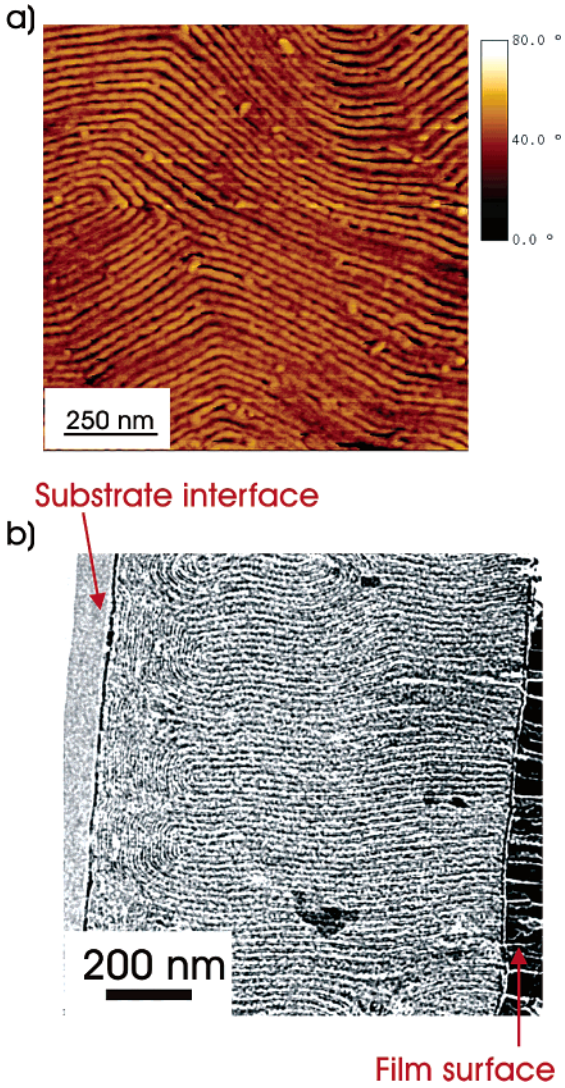

Figure 8. (a) Tapping mode SFM phase image and (b) cross-sectional TEM image of a symmetric blend $CECEC_{66.48}/CE_{22.48}$ annealed at 220 °C for 3 days.

alternate layers, macroscopic neck formation prevails during tensile deformation, and the glassy PS layers undergo large plastic yielding.[24,25] Up to the strains accessible in our fragility tests, the major deformation mechanism observed in $CEC_{45.48}$ and $CECEC_{66.48}$ is shear yielding, which corroborates the hypothesis that the glassy C phase undergoes large plastic deformation and the triblock and pentablock behave in a ductile thermoplastic manner. It should be mentioned here that Hermel et al.[17] observed dramatic differences in the fracture behavior of lamellar bulk CEC and CECEC block copolymers. They observed that the pentablock copolymer exhibited an enhanced ductility and tougher mechanical behavior as compared to the triblock copolymer. However, in their studies, the strain was applied normal to the lamellae normal. In our film samples, the lamellar sheets are oriented perpendicular to the film plane. However, since there is no preferred orientation in the plane of the film and the grain size for any specific orientation is only a few lamellar layers thick, there is no clear path for crack propagation through the glassy PCHE lamellae, and incorporation of the ductile PE phase in the path of the propagating crack is effectively accomplished. When randomly oriented microdomains are stretched in tension, the glassy C blocks prevent chain pullout and the E block yields (as observed by Hermel et al. for the pentablock copolymer[17] and corroborated by our TEM images in Figure 5b,c).

The diblock copolymer deforms predominantly by crazing at the onset of the test. The median strain to plastic deformation for the diblock is about 1% (Figure 6a). The crazes are characterized by a coarse microstructure and local fibril breakdown inside the craze (Figure 5a). The $CE_{22.48}$ film exhibits 100% failure at strains of 5% with a median strain to failure of 3% (Figure 6b). The failure initiates in grid squares by macroscopic voiding immediately after the onset of plastic deformation. The mechanical behavior is similar to that of the PCHE homopolymer.[15] It should be noted that despite the fact that the diblock has a composition similar to the triblock and the pentablock, it shows a low resistance to failure due to craze formation and breakdown at small strains. The brittle behavior of $CE_{22.48}$ is attributed to its diblock architecture. Matsuo et al. observed a similar behavior in SB diblock copolymers where the PB block formed cylinders in a PS matrix.[8] Despite the high content of the ductile E phase and the favorable orientation of the lamellar sheets (parallel to the applied strain) in $CE_{22.48}$, the lack of sufficient physical cross-linking for the E block due to the absence the glassy C block at one end as well as the short PE block length (11 kg/mol) facilitates chain pullout from

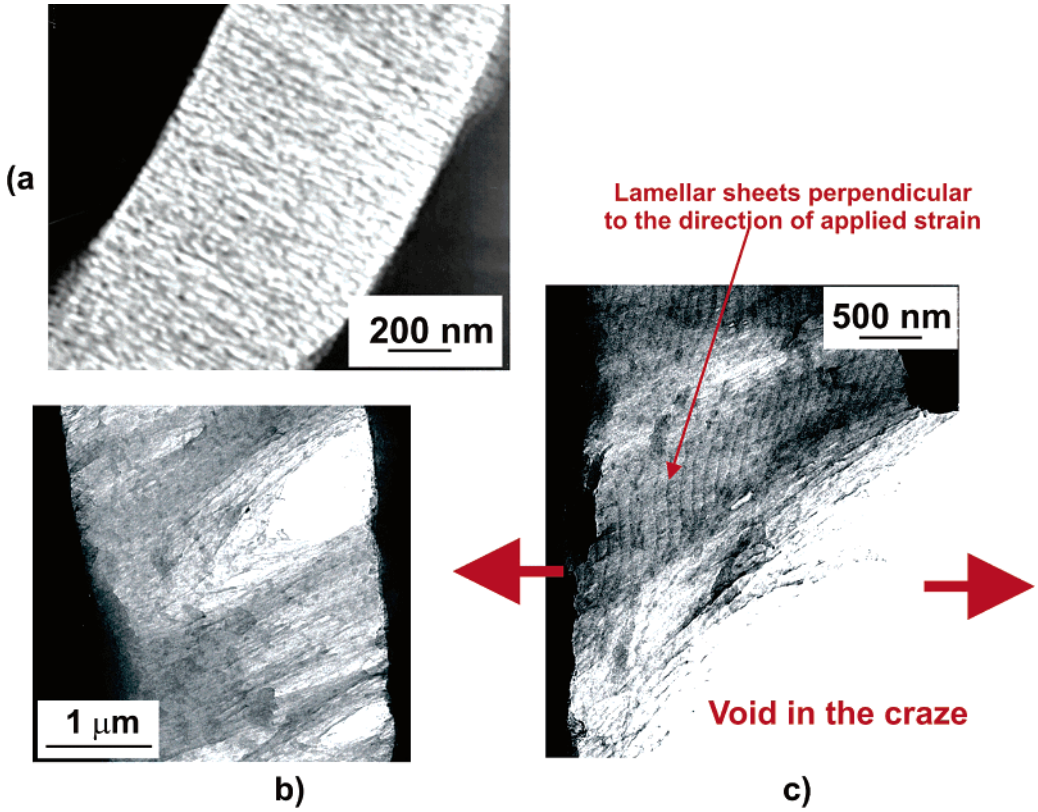

Figure 9. TEM images of typical deformed regions in (a) $CECEC_{66.48}/CE_{22.48}$ at 10% strain and (b, c) $CEC_{45.48}/CE_{22.48}$. Image b shows a region of local fibril breakdown at the craze film interface at a strain of 6%. Image c shows a region of macroscopic failure in the blend at a strain of 8%. Note that at the craze void interface the orientation of the lamellar sheets is perpendicular to the strain direction (indicated by the arrows).

the PE lamellae during craze formation and widening in the fragility test. As a result, the diblock copolymer merely fails in a brittle fashion.

The above results clearly highlight the differences between the brittle diblock architecture and the ductile triblock and pentablock architecture. However, the results are not useful when a comparison between the triblock and the pentablock architecture is required. A different set of experiments was performed in order to distinguish the fracture behavior of the triblock and the pentablock architecture. These experiments are discussed in the following section.

Mechanical Behavior of Symmetric Blends: $CEC_{45.48}/CE_{22.48}$ ($f_{CE} = 0.5$) and $CECEC_{66.48}/CE_{22.48}$ ($f_{CE} = 0.5$). The fragility test does not give any useful information beyond strains of 27%. Since no failure is observed for both the triblock and the pentablock at the end of the test (as is discussed in the previous section), the mechanical behavior of the two architectures could not be distinguished. To allow differences to be observed, the triblock and the pentablock were blended with the brittle diblock copolymer. It has been reported that the strategy worked for blends of cylinder[15] and lamellar[18] forming triblock and pentablock copolymers. In our study the blends were composed of equal weight fractions of the two architectures ($f_{CE} = 0.5$). Figure 7 and Figure 8 show SFM and cross-sectional TEM micrographs of the $CEC_{45.48}/CE_{22.48}$ and $CECEC_{66.48}/CE_{22.48}$ blends, respectively, after a 3 day anneal. The morphology is lamellar. The predominant microdomain orientation is perpendicular to the film plane. However, for both of the blends, parallel lamellar sheets at the bottom of the film are observed. We believe that further annealing will produce complete perpendicular orientation throughout the film thickness, as is observed in the individual CEC and CECEC block copolymers.

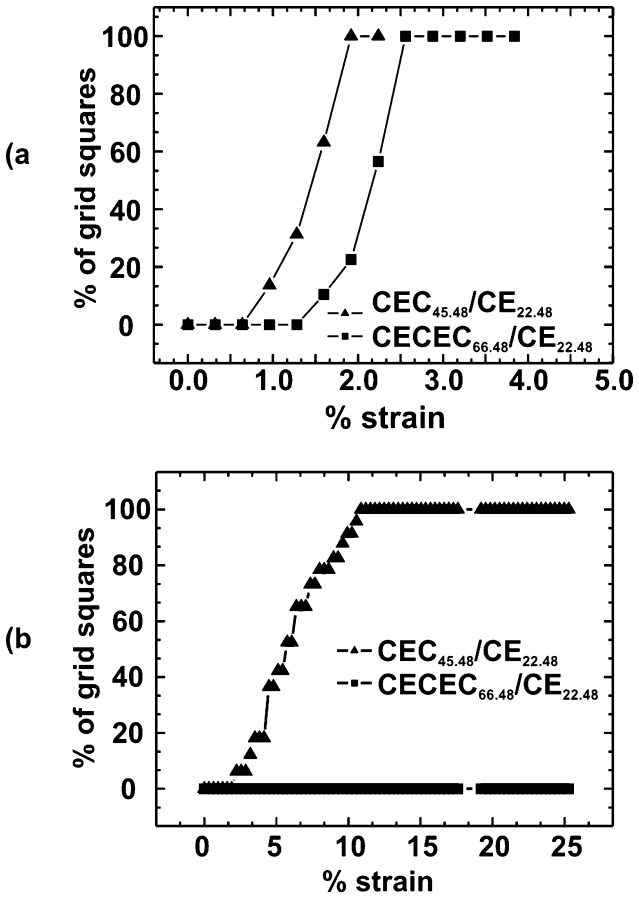

Figure 10. Cumulative number fraction of film squares that have (a) crazed and (b) failed as a function of strain for $CEC_{45.48}/CE_{22.48}$ and $CECEC_{66.48}/CE_{22.48}$.

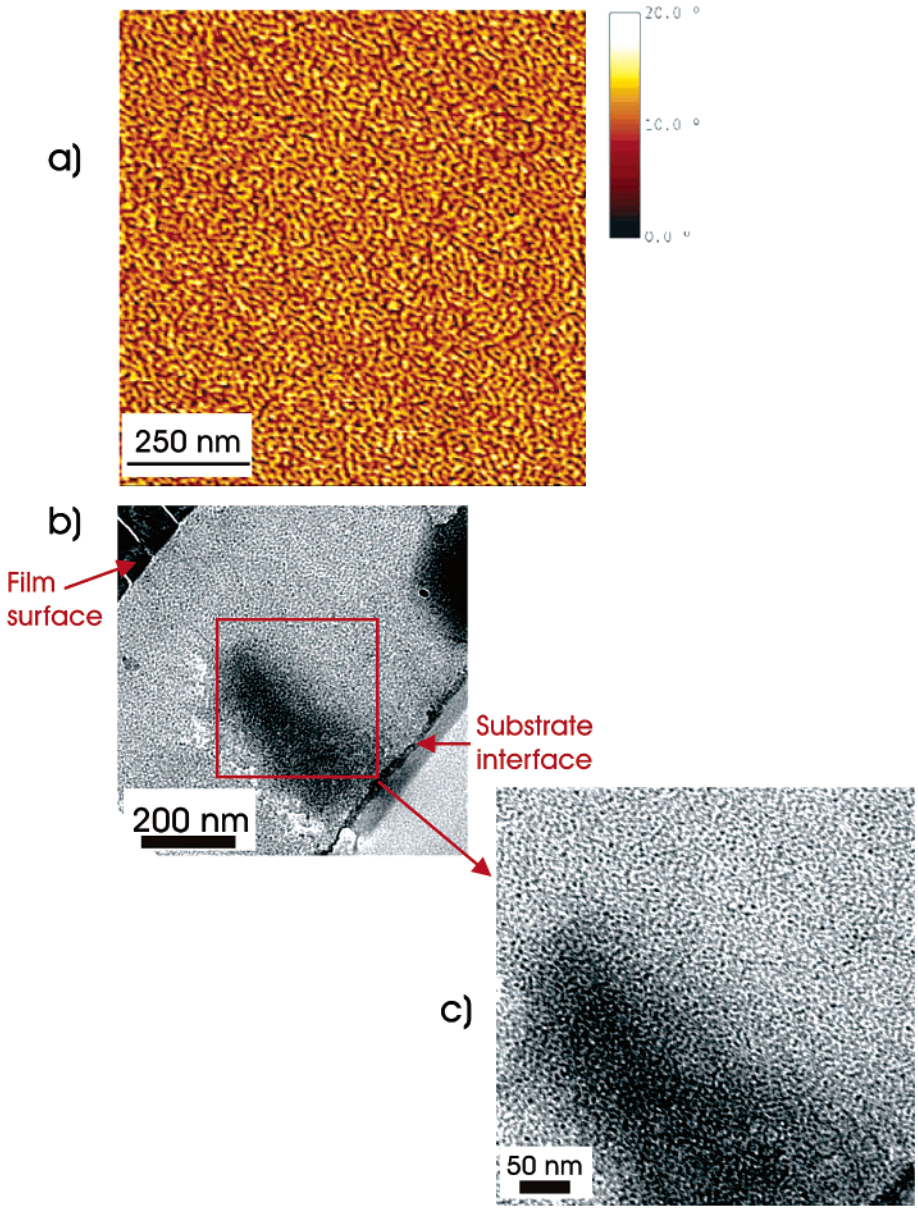

Figure 11. (a) Tapping mode SFM phase image and (b, c) cross-sectional TEM image of a 600 nm spun-cast $CECEC_{60.25}$ film. The film shows very poor ordering with a random orientation of the PE cylinders.

Table 2. Median Strain to Failure, Total Failure, and Deformation Mechanism for Lamellar Block Copolymers

polymer	median strain to failure (%)	% failure	deformation mechanism
$CE_{22.48}$	2	100% at 5% strain	crazing
$CEC_{45.48}$	>27	no failure	deformation zones
$CECEC_{66.48}$	>27	no failure	deformation zones
$CECEC_{45.48}/CE_{22.48}$	6.4	100% at 11% strain	crazing
$CECEC_{66.48}/CE_{22.48}$	>27	no failure	crazing

The deformation mechanisms and the deformation and failure statistics for the $CEC_{45.48}/CE_{22.48}$ and $CECEC_{66.48}/CE_{22.48}$ blends are more indicative of the differences in the fracture behavior of the triblock and the pentablock architecture as well. The $CECEC_{66.48}/CE_{22.48}$ blend deforms plastically at a median strain of 2% (Figure 10a), and the predominant deformation mechanism is crazing (Figure 9a). The craze extension ratio for the $CECEC_{66.48}/CE_{22.48}$ blend was calculated to be about 4.0. The changes in the deformation mechanisms and the craze extension ratios for the blend as compared to the individual block copolymer (which deforms predominantly by shear) suggest that the blending strategy worked and the diblock architecture was responsible for this transition; the 50% content of the brittle CE block copolymer initiates voiding in the deformed regions and hence the blend crazes. However, the blend shows failure statistics that are similar to the original $CECEC_{66.48}$ block copolymer; i.e., no failure is observed up to the end of the test (Figure 10b). The reason for this ductile behavior is the architecture of the pentablock copolymer. The presence of a bridging C midblock between two soft E blocks in the pentablock provides a way of transferring stress from one soft E block to the other, thereby making it possible for the stable craze fibrils to form within the E domains. Hence, despite the high fraction of the diblock copolymer in the blend, the pentablock still behaves in a ductile manner due to the midblock bridging.

The $CEC_{45.48}/CE_{22.48}$ blend deforms at a median strain of 1.4% (Figure 10a). The blend deforms predominantly by crazing with a craze extension ratio of about 4.2, which compares well with the extension ratios calculated for a CEC cylinder forming triblock copolymer ($CEC_{107.29}$, $\lambda = 4.3$[15]). Moreover, pear-

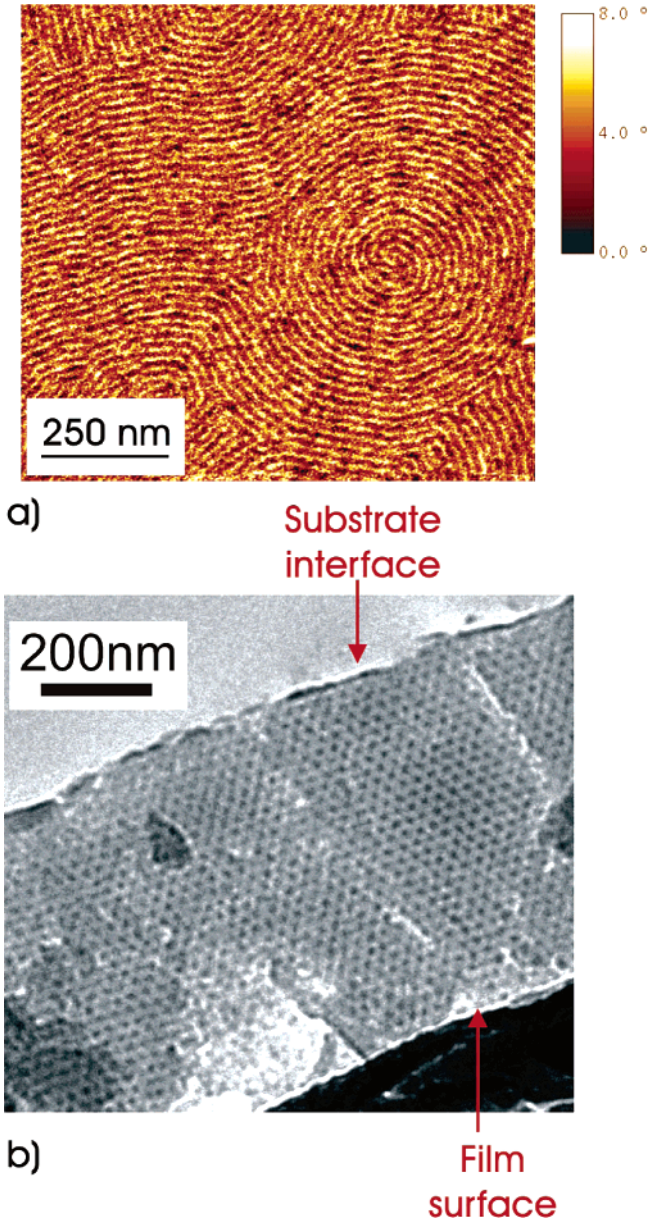

Figure 12. (a) Tapping mode SFM phase image and (b) cross-sectional TEM image of a 600 nm $CECEC_{60.25}$ film annealed at 180 °C for 3 days.

shaped void formation at the craze film interface was also frequently observed (Figure 9b), which ultimately causes macroscopic failure of the film. The blend films show 100% failure at a strain of 10% with a median strain to failure of 6.4% (Figure 10b). The triblock does not have a C midblock that would enable the transfer of stress from one soft E layer to the other. The substantial loss in ductility of the blend over that of the individual lamellar CEC block copolymer is due to the absence of the midblock, exacerbated by the addition of 50% diblock copolymer in the blend. The orientation of the lamellar sheets in the film plane is random with grain sizes that are only a few layers thick. Since diblock copolymer films undergo brittle failure regardless of their domain orientation and, in the absence of the midblock bridging, the triblock copolymer chains that are perpendicular to the applied strain are also susceptible to failure (Figure 9c shows one such region), voids in the crazes can grow to initiate macroscopic failure through the glassy PCHE block in these regions. The voids initiate at the craze film interfaces (Figure 9b) and eventually cause failure of the film through the glassy PCHE matrix. Table 2 summarizes the results for the lamellar block copolymers.

Effect of Microdomain Orientation on the Mechanical Behavior of a Cylindrical Pentablock Copolymer. Previous papers on cylinder-forming poly(cyclohexylethylene)−poly(ethylene) block copolymers have described the effect of chain architecture (homopolymer, triblock, and pentablock)[15] and microdomain orientation in triblock copolymer films.[16] In the following sections, experiments were carried out that aimed to understand the effect of microdomain orientation in a cylinder-forming pentablock copolymer. The studies were possible due to the slow ordering kinetics of $CECEC_{60.25}$ where the orientation of the PE cylinders in the films underwent a change from random to parallel to perpendicular with increasing annealing time.

Block Copolymer Morphology and Microdomain Orientation. SFM and cross-sectional TEM images of the block copolymer films for three different heat treatments are reported; an as-cast sample, a sample annealed for 3 days, and a sample annealed for 7 days. The as-cast sample clearly shows a cylindrical morphology. The PE cylinders, however, show only very short range order, as illustrated in Figure 11. After annealing for 3 days, the ordering is more pronounced. Cross-sectional TEM shows that cylinders are oriented with their axes parallel to the film interfaces (Figure 12). Annealing the films for 7 days results in a reorientation of the microdomains. We observe that a large fraction of the cylinders are oriented with their axes perpendicular to the film surfaces. The perpendicular orientation seems to initiate from the air−film interface and propagates through the thickness of the film, as shown in Figure 13. However, since the sample did not have microdomains that were aligned perpendicular throughout the film thickness, complete unambiguity on the effect of microdomain orientation would be lacking without investigating films in which the perpendicular orientation persisted throughout the film thickness. To obtain conclusive proof for this effect of microdomain orientation, one more sample was prepared. Since cylinders in the top half of the 600 nm thick film are oriented perpendicular to the surface after a 7 day anneal, a film 300 nm thick was prepared and annealed for 7 days to obtain the perpendicular orientation throughout the film thickness. As shown in Figure 14a,b, the desired orientation was achieved in the thinner film.

Previous studies have shown that for the PCHE−PE cylinder forming triblock copolymers the microdomains orient perpendicular to the film interfaces.[16] This behavior is also observed in the lamellar triblock and pentablock block copolymers, as described in the previous sections. This unusual behavior for the PCHE−PE system is attributed to the similarities in the surface energies of the C and the E blocks. In the case of the cylindrical pentablock copolymers, however, the kinetics of microdomain ordering is slower than that for the triblock copolymers with similar M_W. A triblock copolymer $CEC_{50.25}$, when annealed at 190 °C for 1 day, has the PE cylinders aligned perpendicular to the film interfaces throughout the thickness of the film.[16] However, the pentablock copolymer under investigation, $CECEC_{60.25}$, does not show the perpendicular orientation of the cylinders after annealing for 3 days at 180 °C. Ryu et al. observed a similar trend for higher M_W $CEC_{107.29}$ and $CECEC_{110.30}$ block copolymers.[15] The microdomains showed poor organization for the pentablock architecture in comparison to the triblock architecture. We believe that, due to the complex architecture of the pentablock copolymers, the kinetics of orientation

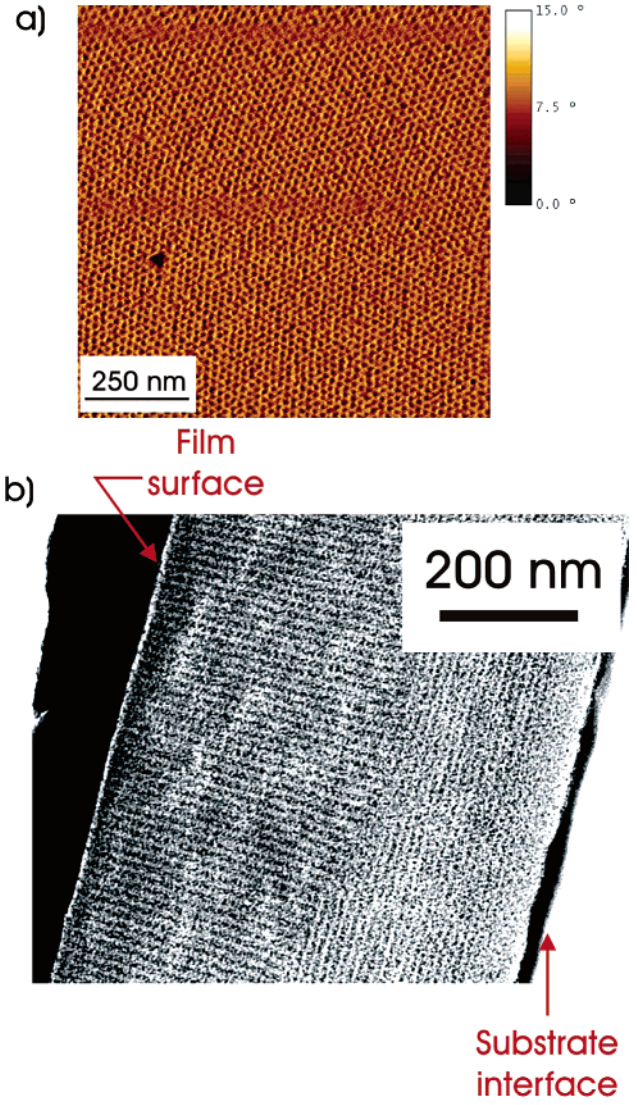

Figure 13. (a) Tapping mode SFM phase image and (b) cross-sectional TEM image of a 600 nm $CECEC_{60.25}$ film annealed at 180 °C for 7 days.

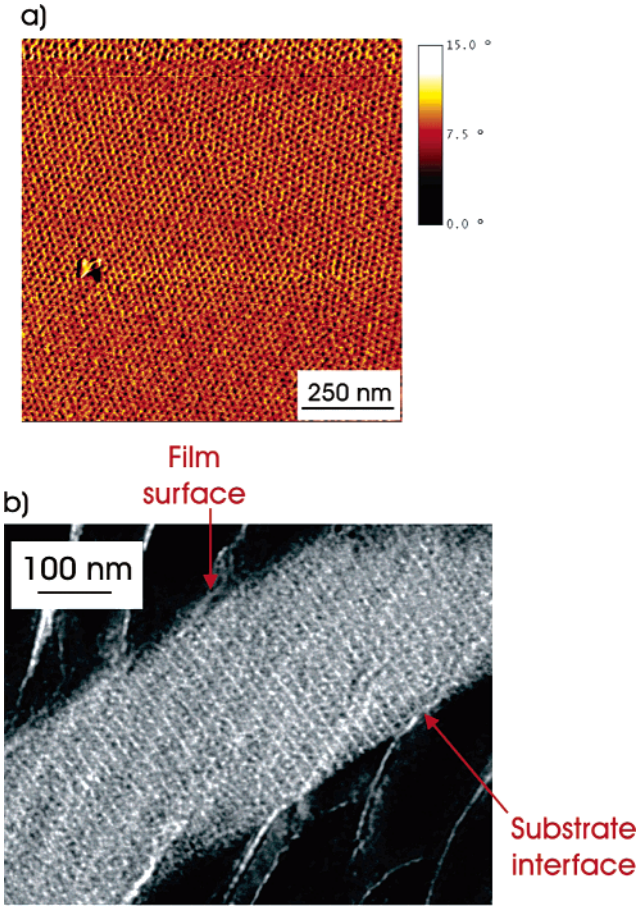

Figure 14. (a) Tapping mode SFM phase image and (b) cross-sectional TEM image of a 300 nm $CECEC_{60.25}$ film annealed at 180 °C for 7 days.

ordering are slower as compared to the triblock copolymer, and the poor organization of the microdomains may be a kinetically trapped configuration. Also, the annealing temperature (180 °C) for the pentablock copolymer is in close proximity to both the order−disorder transition temperature of the block copolymer (190 °C) and the T_g of the glassy block (145 °C). Hence, the smaller annealing temperature window available for the pentablock copolymer relative to the triblock copolymer may also result in a slower organization of the microdomains.

Craze Microstructure and Extension Ratios. Differences are also observed in the mechanism of deformation for the four samples. The predominant mechanism of deformation for 3 day annealed and 7 day annealed samples was crazing (Figure 15b−d). The craze microstructure is characterized by small main fibrils that are interconnected by short cross-tie fibrils embedded in a continuous void space. However, for the 7 day annealed samples (300 and 600 nm thick), we observe a large number of pear-shaped voids at the craze film interface that eventually grow as subcritical cracks as the film is further strained (Figure 15c,d). The as-cast samples also exhibited crazing as the main deformation mechanism. However, crazes coexisting with shear deformation zones were observed frequently (Figure 15a). At higher strains, the crazes did not exhibit further voiding at the craze film interface. This coexistence of shear deformation zones and crazes further suggests that the ductile PE phase is incorporated most effectively for the as-cast random morphology. This effective incorporation of the highly entangled PE phase probably raises the crazing stress above the shear deformation stress, thereby making it easier for the films to deform by shear than by crazing.[1,26]

All the images analyzed were for crazes at strains of about 10%. The craze extension ratios of 4.1 for the four samples were identical within experimental error. This is not too surprising considering the fact that the samples have the same composition, molecular weight, and architecture. The extension ratio of the shear deformation zones for the as-cast sample was calculated to be around 3.4 for $CECEC_{60.25}$. Ryu et al. observed a craze extension ratio of 3.9 for $CECEC_{110.30}$ and 4.3 for $CEC_{107.29}$.[15] For the shear deformation zones for $CECEC_{110.30}$, they observed a value of 3.1. The pentablock architecture for both the 60 and 110 kg/mol block copolymers shows a lower λ_{craze} relative to the triblock architecture. This implies that the enhanced toughness of the pentablock architecture due to the bridging C block between the two soft E blocks, as hypothesized by Ryu et al.,[15] is evident even when the M_W of the CECEC (60 kg/mol) is reduced to almost half of that of the CEC block copolymer (107 kg/mol).

Deformation and Fracture Statistics. The deformation statistics for the three 600 nm thick films were determined using the fragility tests. All the samples undergo plastic deformation prior to fracture. As can be seen in Figure 16a, the median strain for the onset of plastic deformation is about 2.5% for the as-

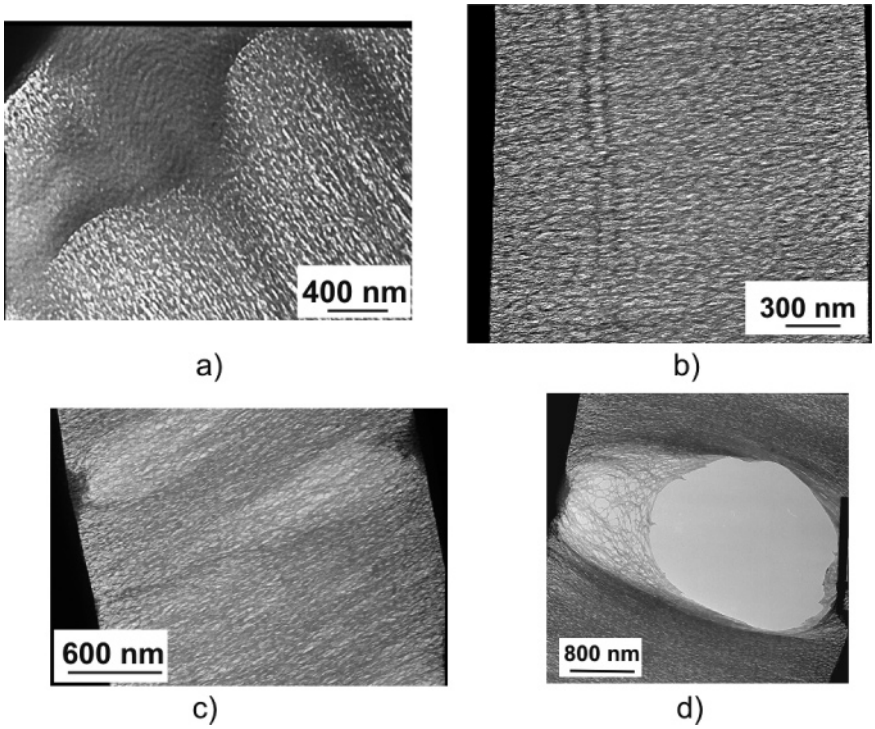

Figure 15. Transmission electron micrographs of plastically deformed regions in $CECEC_{60.25}$ films. (a) A craze with a region of shear deformation in a spun-cast film. (b) A typical craze in a film annealed for 3 days. (c) A typical craze in the 600 nm thick film annealed for 7 days. Formation of large pear-shaped voids at the craze film interface is observed. (d) The voids cause local failure in the craze and eventually grow as subcritcal cracks. The image is of a typical craze in the 300 nm thick film annealed for 7 days. TEM images a−c were taken at 10% strain. Image d was taken at 15% strain.

Table 3. Median Strain to Failure, Total Failure, and Deformation Mechanism as a Function of Microdomain Orientation for $CECEC_{60.25}$

microdomain orientation	median strain to failure (%)	% failure	deformation mechanism
as-cast 600 nm film random, Figure 11	>27	no failure	DZ + crazing
3 day anneal 600 nm film lying down, Figure 12	>27	30% at test end	crazing
7 day anneal 600 nm film mixed, Figure 13	19	100% at 25.6 strain	crazing
7 day anneal 300 nm film standing up, Figure 14	15.7	100% at 22.3% strain	crazing

cast sample and is between 1% and 1.5% for the samples annealed for 3 and 7 days. The deformation statistics for the 300 nm film annealed for 7 days are identical to those of the 600 nm film annealed for 7 days and hence are not included in Figure 16a.

Figure 16b shows the fragility test results for failure statistics. The median strain to fracture also showed considerable differences for the four different samples. The as-cast sample did not show any failure until the end of the test (i.e., when the Cu grid fails at strains of about 27%). 30% of the grid squares failed by the end of the test for the sample that was annealed for 3 days. However, the two samples with different thicknesses that were annealed for 7 days showed 100% failure by the end of the test. The median strain to failure for the 600 nm film was about 19% and for the 300 nm film was 15.7%.

As described earlier, the only difference that exists in the four samples is in the microstructure. Previous work on the CEC triblock copolymers has shown that if the microdomains are either aligned randomly or parallel to the direction of applied strain, the block copolymer exhibits ductile behavior since the orientation is more effective in incorporating the ductile polyethylene domains in the craze fibril structure and hence the path of the advancing crack.[16] However, if the cylinder axes are oriented perpendicular to the film interfaces and hence transverse to the direction of strain, brittle behavior was observed since craze fibril failure and large void formation initiated in the unentangled C end blocks. We believe that the pentablock

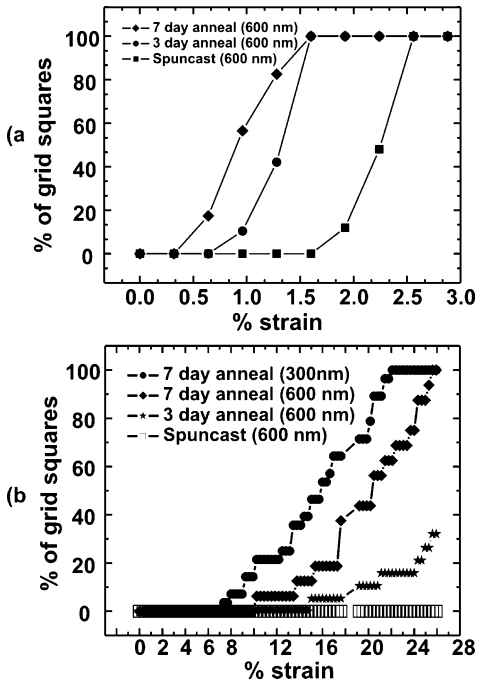

Figure 16. Cumulative number fraction of film squares that have (a) crazed and (b) failed as a function of strain for $CECEC_{60.25}$ films that were as-cast, annealed for 3 days, and annealed for 7 days. The failure statistics for the 300 nm film annealed for 7 days (Figure 12) is also included in (b) for comparison.

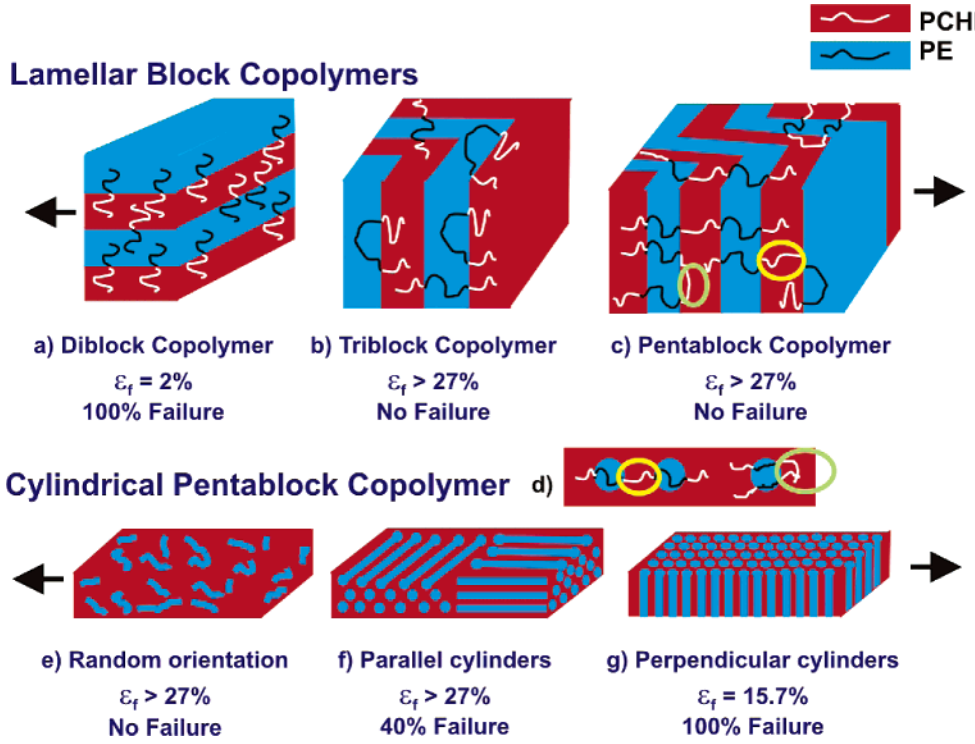

Figure 17. Schematic summarizing the effect of chain architecture in lamellar block copolymers (a, b, c) and microdomain orientation in a cylindrical pentablock copolymer (e, f, g). The black arrows indicate the direction of strain. ϵ_f is the median strain to failure. (a) Lamellar diblock copolymer film. The lamellae are oriented parallel to the direction of strain. (b) Lamellar triblock copolymer film. (c) Lamellar pentablock copolymer film. In (b) and (c), the lamellae are oriented perpendicular to the substrate and surface. The orientation is random in the film plane. (d) Cylindrical pentablock copolymer film with (e) a random orientation of cylinders, (f) grains of cylinders aligned with their axes parallel to the film plane, and (g) cylinders aligned with their axes perpendicular to the film plane. Parts c and d show bridging (yellow circle) and looping (green circle) PCHE chains in the lamellar and cylindrical pentablock copolymers.

architecture exhibits the same kind of behavior. For the spun-cast sample, the pure random orientation of the microdomains relative to the tensile strain direction ensures effective incorporation of the E domains in the deforming region. The 3 day annealed sample has cylinders with axes that are predominantly parallel to the film interfaces, but not all are parallel to the direction of tensile strain. Hence, when subjected to a tensile strain, voiding and cracking within the PCHE matrix may occur relatively easily. The 600 nm thick film that was annealed for 7 days has a large fraction of microdomains where the cylindrical axes are perpendicular to the film interfaces and hence transverse to the direction of the strain. Hence, the film is even more susceptible to the failure mechanism that has been described above. The reduction in the ductility of the 300 nm thin film over the 600 nm thick film, for the same annealing time of 7 days, is due to the presence of the unfavorable perpendicular orientation throughout the film thickness in the former. The 600 nm thick film annealed for 7 days still exhibits a parallel orientation of the cylinders near the substrate interface which contributes to the slightly improved fracture statistics over the 7 day annealed 300 nm film. The failure statistics of this sample are plotted along with the data for the thicker films in Figure 16b. Hence, the orientation of the microdomains also affects the mechanical behavior of the tough pentablock architecture. However, the effect is not as pronounced for the pentablock copolymer as it is for the triblock copolymer with comparable M_W. A 50 kg/mol CEC triblock copolymer with cylinders oriented perpendicular to the film plane throughout the film thickness shows a median strain to failure of about 1%,[16] whereas a similarly oriented 60 kg/mol CECEC pentablock copolymer has a relatively high median strain to failure of about 15.7%. Table 3 summarizes the results for this cylindrical pentablock copolymer.

Conclusions

For the lamellar block copolymers, chain architecture has a strong effect on their fracture behavior. The triblock and pentablock architectures exhibit a tough and ductile response to tensile testing due to the high content of the ductile E phase and the glassy C blocks at ends that act as physical cross-links for the ductile E phase. Despite the favorable orientation of the lamellar sheets in the diblock copolymer, it exhibits quite brittle behavior. The triblock copolymer cannot sustain its high median strain to failure when it is diluted with the diblock copolymer chains. The toughness of the pentablock copolymer is preserved despite the addition of the brittle diblock architecture due to the presence of a bridging C midblock between the soft E layers. The mechanical behavior of a cylinder-forming pentablock copolymer (CECEC) is affected by the orientation of the cylindrical microdomains. A disordered structure with a random orientation of the cylinders leads to a ductile behavior. The ductility of the block copolymer film decreases considerably as the fraction of cylinders oriented perpendicular to the direction of strain is increased, and a film with perpendicularly aligned cylinders throughout the thickness shows the lowest median strain to failure. An easy path for crack propagation through the brittle PCHE phase is responsible for the fracture behavior of the perpendicular orientation. However, the highly oriented CECEC film still has a much larger median strain to failure than a similarly oriented CEC block copolymer with a comparable M_W. This shows that the bridging C midblock in the pentablock architecture is primarily responsible for the differences in toughness between the CEC and CECEC block

copolymers. The conclusions for the lamellar and cylindrical block copolymers are summarized schematically in Figure 17.

Acknowledgment. The authors thank Prof. Glenn Fredrickson, Jason Benkoski, and Alexander Hexemer for useful discussions. The work was supported by a gift from Dow Chemical Co. This work made use of MRL Central Facilities supported by the MRSEC Program of the National Science Foundation under Award DMR05-20415.

References and Notes

(1) Kramer, E. J.; Berger, L. L. *Adv. Polym. Sci.* **1990**, *91/92*, 1.
(2) Henkee, C. S.; Kramer, E. J. *J. Mater. Sci.* **1982**, *17*, 1871.
(3) Seymour, R. B. *Adv. Chem. Ser.***1989**, *222*, 3.
(4) Khanarian, G. *Polym. Eng. Sci.* **2000**, *40*, 2590.
(5) Bates, F. S.; Fredrickson, G. H. *Phys. Today* **1999**, *52*, 32.
(6) Bates, F. S.; Fredrickson, G. H. *Annu. Rev. Phys. Chem.* **1990**, *41*, 525.
(7) Matsen, M. W.; Bates, F. S. *Macromolecules* **1996**, *29*, 1091.
(8) Matsuo, M.; Ueno, T.; Horino, H.; Chujyo, S.; Asai, H. *Polymer* **1968**, *9*, 425.
(9) Weidisch, R.; Stamm, M.; Michler, G. H.; Fischer, H.; Jerome, R. *Macromolecules* **1999**, *32*, 742.
(10) Weidisch, R.; Ensslen, M.; Michler, G. H.; Fischer, H. *Macromolecules* **1999**, *32*, 5375.
(11) Weidisch, R.; Schreyeck, G.; Ensslen, M.; Michler, G. H.; Stamm, M.; Schubert, D. W.; Budde, H.; Horing, S.; Arnold, M.; Jerome, R. *Macromolecules* **2000**, *33*, 5495.
(12) Weidisch, R.; Laatsch, J.; Michler, G. H.; Arnold. M.; Schade, B.; Fischer, H. *Macromolecules* **2002**, *35*, 6585.
(13) Adhikari, R.; Michler, G. H. *Prog. Polym. Sci.* **2004**, *29*, 949.
(14) Bates, F. S.; Fredrickson, G. H.; Hucul, D.; Hahn, S. F. *AIChE J.* **2001**, *47*, 762.
(15) Ryu, C. Y.; Ruokolainen, J.; Magonov, S. N.; Hahn, S. F.; Fredrickson, G. H.; Kramer, E. J. *Macromolecules* **2002**, *35*, 2157.
(16) Ruokolainen, J.; Ryu, C. Y.; Magonov, S. N.; Hahn, S. F.; Fredrickson, G. H.; Kramer, E. J. *Macromolecules* **2002**, *35*, 9391.
(17) Hermel, T. J.; Hahn, S. F.; Chaffin, K. A.; Gerberich, W. W.; Bates, F. S. *Macromolecules* **2003**, *36*, 2190.
(18) Mori, Y.; Lim, L. S.; Bates, F. S. *Macromolecules* **2003**, *36*, 9879.
(19) Hucul, D. A.; Hahn, S. F. *Adv. Mater.* **2000**, *12*, 1855.
(20) Magonov, S. N.; Reneker, D. H. *Annu. Rev. Mater. Sci.* **1997**, *27*, 175.
(21) Brown, H. R. *J. Mater. Sci.* **1979**, *14*, 237.
(22) Lauterwasser, B. D.; Kramer, E. J. *Philos. Mag.* **1979**, *39A*, 469.
(23) Brown, G. M.; Butler, J. H. *Polymer* **1997**, *38*, 3937.
(24) Sakurai, S.; Aida, S.; Okamoto, S.; Ono, T.; Imaizumi, K.; Nomura, S. *Macromolecules* **2001**, *34*, 3672.
(25) Kawai, H.; Hashimoto, T.; Miyoshi, K.; Uno, H.; Fujimora, M. *J. Macromol. Sci.* **1980**, *B17*, 427.
(26) Donald, A. M.; Kramer, E. J. *J. Mater. Sci.* **1982**, *17*, 1871.

MA060460Y